Molecular BioSystems

Accepted Manuscript

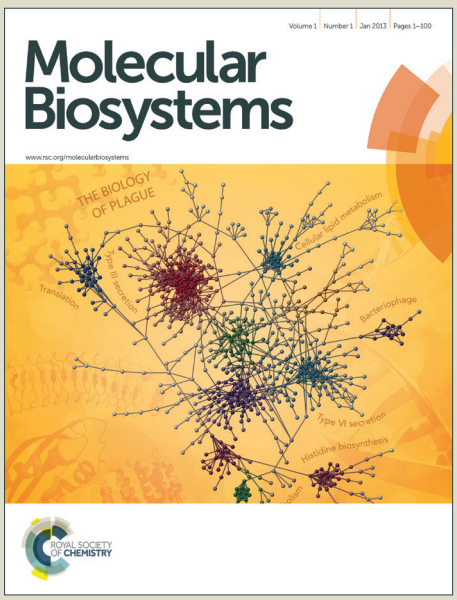

ROYAL SOCIETY OF CHEMISTRY

www.rsc.org/molecularbiosystems

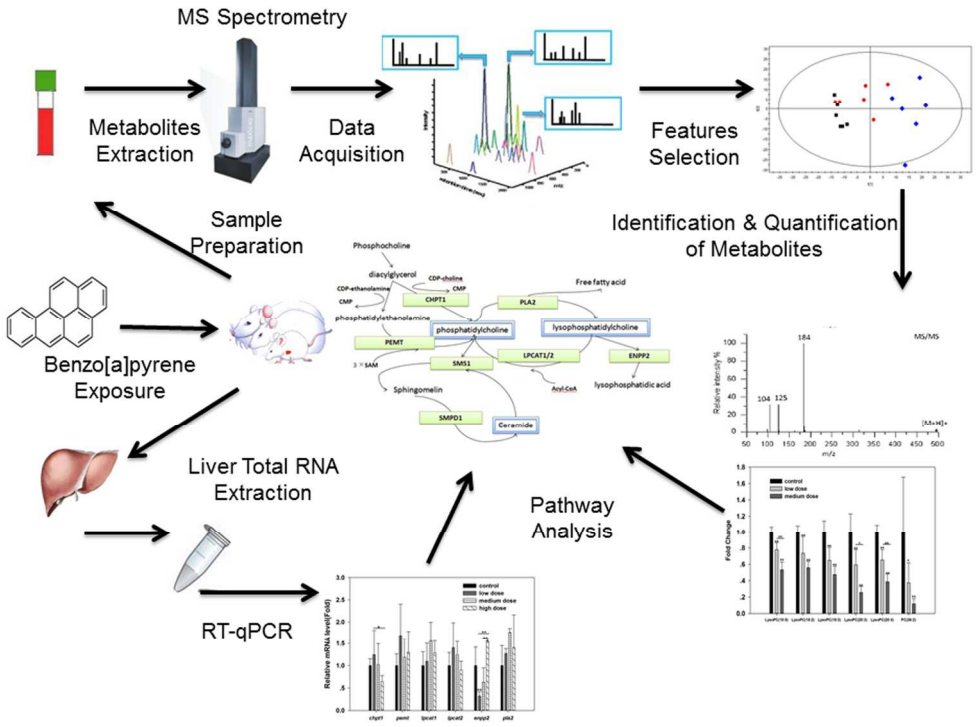

190x142mm (300 x 300 DPI)

Serum metabolomics analysis reveals oral exposure to benzo(a)pyrene impaired lipid metabolism in rats

Xiaoxue Wang, Jie Zhang*, Qingyu Huang, Ambreen Alamdar, Meiping Tian, Liangpo Liu, Heqing Shen*

Key Lab of Urban Environment and Health, Institute of Urban Environment, Chinese Academy of Sciences, Xiamen, PR China, 361021

*To whom correspondence may be addressed:

Prof. Jie Zhang, Institute of Urban Environment, Chinese Academy of Sciences, 1799 Jimei Road, Xiamen, 361021, China; Tel/Fax: (86)-592-6190523; E-mail: jzhang@iue.ac.cn

Prof. Heqing Shen, Institute of Urban Environment, Chinese Academy of Sciences, 1799 Jimei Road, Xiamen, 361021, China; Tel/Fax: (86)-592-6190997; E-mail: hqshen@iue.ac.cn

Running title: Serum metabolomics analysis of B(a)P-exposed rat

Short Abstract for Table of Contents

Environmental benzo(a)pyrene (B(a)P) exposure has been associated with a diverse adverse health effects. However, the impact of B(a)P exposure on metabolic network remains obscure. In this metabolomics study, twelve differential metabolic biomarkers were identified in the serum of B(a)P-exposed rats by using ultra-high performance liquid chromatography/mass spectrometry. Our results indicated B(a)P exposure significantly disrupted global lipid metabolism in the rats. These findings may provide useful insights into the mechanisms of B(a)P-mediated toxicity.

ABSTRACT: Benzo(a)pyrene (B(a)P) is ubiquitously present in the environment. Although its multiple toxicities had been reported, the impact of B(a)P exposure on metabolic network remained obscure. In this study, an ultra-high performance liquid chromatography/mass spectrometry based metabolomics approach was used to investigate the disruption of B(a)P exposure on global serum metabolic profiles in rat. Sprague Dawley rats were orally exposed to 10, 100 and 1000 μg/kg B(a)P for 32 days consecutively. Distinct serum metabolomic profiles were found to be associated with the doses. Twelve metabolites were identified as potential biomarkers, which indicated B(a)P exposure disrupted global amino acid metabolism and lipid metabolism, especially phospholipid metabolism and sphingolipid metabolism. Serum lysophosphatidylcholines showed dose-dependent decreases, while serum sphingomyelins presented dose-dependent increases. The expressions of some key genes involved in these pathways were also investigated. Expressions of *enpp2, sms* and *smpd* were significantly altered by high dose of B(a)P exposure. Metabolic biomarkers were more sensitive than corresponding gene expression for B(a)P exposure. The findings of this study pointed to novel potential mechanisms in which the identified metabolic pathways involved.

KEYWORDS: benzo(a)pyrene; metabolomics; rat; lipid metabolism; lysophosphatidylcholine

1. INTRODUCTION

Benzo(a)pyrene (B(a)P), a polycyclic aromatic hydrocarbon (PAH), is ubiquitously present in the environment. It is formed by incomplete combustion of organic materials in industrial process, automobile emissions. Humans are unavoidably exposed to B(a)P via the ingestion of contaminated food and water, the inhalation of particulates in the ambient air and cigarette smoking.[1]

B(a)P presents diverse toxicities including hepatotoxicity, neurotoxicity, cytotoxicity, genotoxicity, carcinogenicity and immunotoxicity.[2] A vast number of studies have discussed the mechanisms of B(a)P toxicity. In cells, B(a)P can be metabolized into reactive metabolites via cytochrome P450 (CYP) mediated pathway,[3] and then bind covalently to nucleic acids and proteins, leading to mutation and cell proliferation.[4] A number of studies have proved that B(a)P or its metabolites would lead to ROS generation and lipid peroxidation.[5, 6] Recently, increasing evidences have shown that B(a)P might disrupt estrogen receptor activity, testicular steroidogenesis and epididymal function *in vivo* and *in vitro*.[7, 8] What's more, endocrine disruption is tightly involved with metabolic disruption through disturbing hormones receptors, intervening peroxisome proliferator-activated receptors (PPAR) and inappropriate activating xenosensors,[9] all of which may be involved in lipid and glucose metabolism. Therefore, we hypothesized that metabolic disruption might be an important mechanism underlying B(a)P toxicity. Moreover, to achieve a comprehensive understanding on B(a)P toxicological effects and mechanisms, a global analysis on the biological responses should be performed at molecular levels

(gene, protein and metabolite).

Omics technologies are capable to acquire the information of global profile, and have been widely used in environmental toxicology. Genomic and proteomic studies have identified several potential B(a)P and other PAHs biomarkers in cells, mice, rats and human.[10-14] However, its influence on global metabolic profiling remained obscure. Metabolic perturbation is often an early event of pollutant induced histopathological change.[15] Metabolomics provides an overview of the metabolic status of a biological system exposed to environmental stress.[16]

A number of metabolomic researches have addressed the adverse effects of B(a)P and other PAHs (e.g. pyrene, phenanthrene, 1,2:5,6-dibenzanthracene) on metabolic response using several model animals *Manila* clam,[17] fish,[18] earthworm.[19-21] However, these non-mammalian models failed to adequately mimic the human response to B(a)P. Rat is obviously a better model in the toxicity study, but so far there is little discussion about systematic metabolic response to B(a)P in rats.

The present study is designed to investigate the adverse effect of B(a)P exposure on global metabolome in rat. An ultra-high performance liquid chromatography/mass spectrometry (UHPLC/MS) based metabolomics approach was used to profile and characterize significantly altered metabolites in the sera of the rats orally exposed to B(a)P. Besides, the expressions of key genes involved in altered metabolism pathway were examined. This study identified the disrupted metabolic pathways associated with B(a)P exposure, and thus led to a more comprehensive understanding of B(a)P toxicity.

2. METHODS

2.1 Chemicals

Benzo(a)pyrene (purity>98.5%) and formic acid (HPLC grade) were purchased from Acros (Morris Plains, NJ, USA). All standards (purity>95%) were purchased from Sigma-Aldrich (St. Louis, Mo, USA). Methanol (HPLC grade) was obtained from Fisher Scientific (Fair Lawn, NJ, USA). Distilled water (18.2 MΩ) was obtained from a Milli-Q system (Beford, MA, USA).

2.2 Animal experiments

A total of 22 Sprague Dawley rats aged six weeks (weight 200 ± 10 g) were obtained from Shanghai Laboratory Animal Center, China. Animals were housed separately by sex in stainless-steel cages and acclimatized for one week before starting B(a)P exposure. Rats were maintained in an air-conditioned room at the temperature of 26 ±2 ^{o}C, a relative humidity of 50 ±5%, and a 12 h light/12 h dark cycle. Each animal had *ad libitum* access to water and pellet diet. All the rats were randomly divided into control and three treatment groups by intragastric B(a)P administration every day. The control group was fed with corn oil. The low, medium and high-dose groups were administered for 32 days with 10, 100 and 1000 μg/kg B(a)P which was dissolved in corn oil, respectively. Although the doses we used were higher than environmental exposure level, they were similar to and even much lower than those used in other peer-reviewed reports on B(a)P.[10, 22, 23] The relatively high dose was used to obtain the adverse effect in rats when human model is unavailable, and it helped elicit a detectable response in experimental animals. All animals were

treated humanely and with regard for alleviation of suffering according to the China Animal Welfare legislation.

2.3 Sample collection and preparation

After being consecutively treated with B(a)P for 32 days, rats were killed by decapitation. Blood was collected from each animal and placed into ice-cold tubes. Serum was obtained by centrifugation (3500 ×g, 10 min at 4 ^{o}C) and frozen at -80 ^{o}C before further sample preparation and analysis. The livers were removed immediately after sacrifice, rinsed with PBS (room temperature), flash frozen in liquid nitrogen and then stored at -80 ^{o}C.

For the pretreatment of the serum samples, a volume of 600 μL cold methanol was added to 200 μL serum and was shaken vigorously, and the mixture was stored for 10 min and subsequently centrifuged at 12,000 ×g for 10 min at 4 ^{o}C. The supernatant was filtered through a 0.22 μm syringe filter prior to UHPLC/MS analysis. From each sample, 20 μL sera were mixed and divided into several aliquots as the quality controls (QCs). The QCs were periodically injected during sample acquisition batch, and used to evaluate the stability and reproducibility of analytical instrument.

2.4 Metabolic profile Acquisition

Serum metabolic profiles were acquired using a UHPLC/orbitrap-MS system (Thermo, USA). A Kinetex C18 column (150 mm× 2.1 mm, 2.6 μm) was used for chromatographic separation. The mobile phase consisted of water containing 0.1% formic acid (mobile phase A) and methanol containing 0.1% formic acid (mobile phase B). A programmed gradient was used: 5% B increased to 100% B in 16 min and

held for 4 min, then decreased to 5% in 0.1 min, and finally maintained at 5% B for 3 min. Sample injection volume was 5 μL. Compared with negative ion mode, more serum metabolites and higher magnitude of the metabolites were detected under positive ion mode (Fig. S1), hence the mass spectrometer was operated in full-scan positive ion mode with a range of 100-1000 m/z. Spray voltage and cone voltage were 3.5 KV and 35 V, respectively. Heated capillary temperature and source temperature were 380 ^{o}C and 350 ^{o}C, respectively. Curtain and auxiliary gas flow were 60 and 35 L/h, respectively. Serum samples were run in a randomized fashion to avoid possible uncertainties from artifact-related injection order and gradual changes of instrument sensitivity in whole batch runs. Because the serum samples of high dose treatment were missing during storage, the samples were not included in metabolome analysis. A QC sample and a blank were analyzed once or twice interval of seven samples to identify the sample carryover and check for stability (n=5). QC samples showed a tight cluster in scoring plot (Fig. S2), suggesting the acquired data had high quality and were worthy of further multivariate statistical analysis. To carry out MS/MS mode to identify potential biomarkers, argon was used as collision gas, and collision energy was adjusted from 15 to 40 eV for each analyte.

2.5 Metabolome analysis

Metabolic raw data were converted into CDF format and then processed by MarkerLynx v4.1 software, which automatically generated a two-dimensional data table of detected variables (m/z, retention time pairs) and their respective intensities (peak areas). Markerlynx parameters were set as follows: mass range 100-1000 m/z,

mass tolerance 0.01 Da, retention time window 0.10 min, and noise elimination level 6. The intensity of extracted variables (spectral bins) was normalized to overall intensities for each sample to remove the unwanted systematic bias and correct for the different enrichment factors of serum among individuals.[24] Hence, the intensity of peak area of each biomarker normalized by sum was expressed as the relative intensity of this biomarker in serum. Any variables with missing values in more than 80% of the samples were excluded according to the "80% rule".[25] The missing values were substituted with 1/2 minimum values prior to multivariate statistical analysis. Finally, the processed data were pareto-scaled and subjected to multivariate statistical analysis using SIMCA-P+ 12.0 software (Umetrics AB, Uppsala, Sweden). Principal component analysis (PCA) was first performed to discover intrinsic treatment-related clusters within the datasets. Partial least squares-discriminate analysis (PLS-DA) was further used to improve separation among the groups and screen potential biomarkers. The robustness and validity of the developed PLS-DA model was tested using a 200-permutation test (Fig. S3). Variable importance in projection (VIP) represents the extracted variables' ability to discriminate different doses. The variables with VIP values > 1.5 were included in the preset of biomarkers. Kruskal–Wallis test was then used to determine which variables were significantly different between all the three groups. The variables with a $p<0.05$ were further subjected to Mann-Whitney test to investigate their changes in either dose group relative to the control. The metabolites which presented significant alteration in either dose group were finally selected as potential biomarkers.

The identification of potential biomarkers was conducted according to our previous reports.[26, 27] Briefly, metabolites were blasted with *m/z* values against the human metabolome database (HMDB: http://www.hmdb.ca/). Top endogenous metabolites provided by the database searching could be potential biomarkers. MS/MS information was further used to confirm the identification (Table S1). If available, the structures of these metabolites were finally confirmed by comparison with commercial standards. Otherwise, the metabolites were tentatively identified by comparing the acquired structure information with metabolite databases and published literature.

2.6 Quantitative real-time PCR

Quantitative real-time PCR was applied to evaluate the expressions of some key genes involved in the lipid metabolism pathway. Total RNA samples were extracted from homogenized liver samples using Total RNA Kit I (OMEGA). Reverse-transcription of cDNA synthesis was performed with 1 μg total RNA using PrimeScript®RT reagent Kit (TaKaRa Bio, Otsu, Japan). Real-time PCR was carried out in a 20 μL final volume and performed in duplicate using SYBR Green Master Mix reagents in a Light cycler 480 detection system (Roche Applied Science, Indianapolis, USA) according to the manufacture's protocol. PCR primers were listed in Table 1. The conditions for quantitative PCR were as follows: 95 ^{o}C for 10 min followed by 40 cycles at 95 ^{o}C for 15 s, and 60 ^{o}C for 60 s. Gene expression levels were normalized to β-actin expression levels. The fold changes (treated/control) of the tested genes were analyzed by the $2^{-\Delta\Delta Ct}$ method.

2.7 Statistical analysis

All analyses were conducted using SPSS Version 18.0 (SPSS Inc., Chicago, USA). The relative intensities of the biomarkers in dose groups were further normalized to the respective controls to provide us with the information of fold change. If data were not normal distributed, nonparametric tests would be carried out to compare between and within groups. In metabolome analysis, Kruskal–Wallis test was used to determine which variables were significantly different among all the three groups, Mann-Whitney test to investigate their changes in either dose group relative to the control group. Normal distributed data were analyzed using one-way ANOVA; LSD or Tamhane test was used based on homogeneity of variances. Significance was set at $p \leq 0.05$.

3. RESULTS

3.1 QC validation

The use of biological QC samples provides an important means of monitoring method performance. In our study, QC samples were analyzed to evaluate the sample carryover, the stability and reproducibility of the present method. After data acquisition and preprocess, there were 631 variables remaining in the dataset. CV values of 63.9% variables were<30%, and the CV values of 48.5% variables were<15% (Fig. S4), indicating our method had excellent repeatability and the dataset is worthy for further analysis.

3.2 Metabolome analysis

The PCA scoring plot allowed a primary separation among groups (Fig. 1A). A

supervised PLS-DA model was further used to discover the difference among groups. The corresponding PLS-DA model with five latent components had a faithful representation of the data (R2X=0.72, R2Y=0.99) and a very good cumulative predictive capacity ($Q2_{(cum)}$=0.76) (Fig. 1B). Furthermore, the medium dose group, low dose group and control group were obviously separated, and the B(a)P group had a sparser cluster than that of control group, perhaps due to different sensitivity to B(a)P of rats in dose groups.

Biomarkers are defined as "putative metabolites responsible for class separation identified using the loadings and variable importance plots" in metabolomics field.[28] In the present study, twelve potential biomarkers were tentatively identified (Table 2), which reflected the impact of B(a)P exposure on metabolic pathways.

Most of these biomarkers were involved in lipid metabolism, including five lysophosphatidylcholines (lysoPCs) and one phosphatidylcholine (PC) (glycerophospholipid metabolism), palmitic amide (fatty acid metabolism), sphinganine, phytosphingosine and cer(d18:0/14:0) (sphingolipid metabolism). In this study, all the five lysoPCs markedly decreased in a dose-dependent manner in all treated groups (Fig. 2). A significant decrease of PC(36:2) was found among all treated groups. We also observed an obvious decrease of cer(d18:0/14:0) in low dose group while an increased concentration of sphinganine and phytosphingosine in medium dose group (Fig. 3). Other biomarkers were cytosine and L-valine, which involved in amino acid and nucleotide metabolism, respectively. And both of them were significantly increased in medium dose group.

3.3 Organ coefficients of liver and expression of key hepatic genes

Liver is relevant in toxicology as the primary organ of metabolism and detoxification for B(a)P.[29] No significant alteration of organ coefficients of liver was observed following B(a)P exposure (Figure S5). The alteration in the expression of key hepatic genes was further investigated. *Chpt1, pemt, pla2, lpcat1, lpcat2* and *enpp2* are prerequisites for glycerophospholipid metabolism (Fig. 4). The expression of *chpt1, pemt, pla2, lpcat1, lpcat2* were not significantly changed upon B(a)P exposure (Fig. S6).The expression of *enpp2* was markedly down-regulated in low dose group and up-regulated in high dose groups (Fig. 5), which featured significant low-dose effect and nonmonotonic dose response to B(a)P .

Sphingomelin (SM) is mainly regulated by sphingomyelin synathase and sphingomyelin phosphodiesterase (Fig. 4). Thus, *sms1* and *smpd2* mRNA levels were also measured in livers. Significant hepatic perturbation of SM metabolism was observed in high dose B(a)P exposure. *Sms1* expression was severely suppressed by 1.86-fold in high dose group, while it changed little in either low or medium dose group (Fig. 5). Expression of *smpd2* showed the similar change as *sms1*, it significantly decreased by 1.96-fold in high-dose group.

4. DISCUSSION

In this study, we observed B(a)P exposure induced the perturbation of global metabolic system, especially lipid metabolism. Several major and essential structural components of membrane lipid bilayers, including lysoPCs and SMs, were identified as potential biomarkers.

PC is a major component of biological membranes. LysoPCs are the intermediate metabolites of PC and they are biologically active lipids regulating a variety of cellular functions. The abnormal levels of lysoPCs may suggest a disturbance of lipid and glucose homeostasis, thus they have been used as a potential diagnostic biomarker in various diseases.[30, 31] In our study, B(a)P exposure caused a down-regulated level of PC and lysoPCs, indicating its ability to disrupt glycerophospholipid metabolism in rats. Liver is the major detoxification organ and target organ of B(a)P exposure, and recently increased risk of hepatocellular cancer was associated with B(a)P exposure.[32] Therefore, we further investigated mRNA expression of several hepatic genes involved in PC homeostasis. PC can be derived from phosphatidylethanolamine through the action of *pemt* or the CDP-choline pathway catalyzed by *chpt*.[33] However, the hepatic *pemt* and *chpt1* expression seemed unchanged by B(a)P exposure. PC is further hydrolyzed by *pla2* to generate lysoPCs and free fatty acid via Land's cycle. LysoPCs are converted back to PC catalyzed by *lpcat1*/2, or it is hydrolyzed by *enpp2* to LPA. In our study, *lpcat1*/2 expressions were not significantly changed after B(a)P treatment. However marked non-monotonic dose-response (NMDR) was observed for *enpp2* at transcriptional level. As a member of endocrine-disrupting chemicals (EDCs), B(a)P has significant low-dose effect and non-monotonic dose responses.[7, 34] EDCs can have effects at low doses that are not predicted by effects at higher doses and vice versa.[35] NMDR has also been reported for the expression of cytochrome P450 (P450s or CYPs),[36, 37] protein expressions and even hormones level in animals exposed to B(a)P.[38, 39] However, the exact

molecular mechanism underlying NMDR of B(a)P exposure remained obscure. Therefore, more efforts are needed to explore the intrinsic causation of low-dose effect of B(a)P. Moreover, *enpp2* is known to stimulate migration of tumor cells, and its overexpression has been associated with a variety of cancers.[40] Previous studies revealed PCBs and other toxic chemicals (e.g. 2-mercaptobenzothiazole, benzyl acetate) might up-regulate *enpp2* expression in human PBMC [35] and Panc-1 cells.[41] In this study, our observation that high dose exposure to B(a)P significantly increased *enpp2* expression may suggest the association between B(a)P intake and cancer risk, but the exact molecular mechanism needs further investigation.

Previous evidence has shown that endothelial cells can degrade extracellular lysoPCs to reduce plasma and tissue levels of these pro-inflammatory lipid molecules.[42] Interestingly, we found serum lysoPCs were more sensitive than corresponding gene expression for B(a)P exposure. A possible explanation of this discrepancy may be the fact that abnormal levels of serum lysoPCs is not exclusively produced in liver, but could also be an injury signal of other organs.[43] Combing these observations, it's reasonable to assume that the disruption of glycerophospholipid metabolism is critical for the final adverse effects of B(a)P exposure, but further experiments are needed to confirm these preliminary findings and investigate in-depth molecular mechanism.

Ceramide and sphinganine are known as the major structural components of the plasma membrane. Decreased serum cer(d18:0/14:0) and increased serum sphinganine suggested B(a)P exposure could induce a disruption of membrane distribution. Tekpli *et al.* and Gorria *et al.* also reported an increase in membrane

fluidity in cell models exposed to B(a)P,[44, 45] supporting our results that B(a)P could affect the membrane composition via disturb the sphingolipid metabolism. Moreover, sphingomyelinases hydrolyze sphingomyelin to bioactive lipids (sphinganine and phytosphingosine), and were down-regulated in presence of PAH.[46] This was also in accordance with our observation.

Amino acid and nucleotide metabolism were also disturbed by B(a)P exposure, which were indicated by changed levels of valine and cytosine. L-valine is one of the branched chain essential amino acids (BCAAs) that particularly involved in energy metabolism. Cytosine is the most important base involved in DNA methylation. B(a)P has been shown to disrupt DNA methylation patterns in zebrafish embryos and breast cells.[47, 48] The accumulation of cytosine in medium dose group may be related to restoration of modified cytosine so that it can replenish cytosine pools after the modified DNA is cut off and resynthesized.[49]

Our study is not without limitation. In this study, our hepatic total RNA extractant derived from various kinds of cells in both centrilobular and peripherpheral zones. It was possible the alterations in gene expression might be diluted and masked by that from non-responding cells. Therefore, more extrapolation studies are required for the assessment of genes expression in various kinds of cells and specific hepatic zones from liver of rats exposed to B(a)P in the future. Besides, the biomarker identified in metabolomics is not exactly the same with the biomarkers used as “prognostic or diagnostic indicators of disease or a sensitive and specific tool for risk assessment”.[50] Though biomarkers here provided potential disturbed

pathways, they did not specifically respond to B(a)P exposure, therefore they could not be used as exposure biomarkers in the risk assessment of B(a)P exposure. Further efforts should aim to discover more specific biomarkers (e.g. B(a)P-receptor binding related gene or protein) for B(a)P exposure.

CONCLUSIONS

In this study, an UHPLC/MS-based metabolomic approach was conducted to investigate serum metabolic alterations in rats exposed to B(a)P. Obvious metabolic differentiation between the dose and control groups was observed. Twelve metabolites were identified as potential biomarkers, including five lysophosphatidylcholines, sphingomyelins, palmitic amide, L-valine and cytosine. The metabolomic results indicated the B(a)P exposure mainly interfered lipid metabolism. Besides, metabolic biomarkers were more sensitive than corresponding gene expression for B(a)P exposure. Overall, this work improves our understanding of B(a)P toxicity in mammals, and this preliminary findings demonstrated the great potential of metabolomics in the toxicity research of B(a)P. Since B(a)P is a widely accepted EDC, it's necessary to apply the metabolomics to implement metabolomics profiling of hormone-related organs such as breast and prostate. Through combining the metabolomics data and RT-PCR data of these organs, we may obtain a global view of toxic mechanism of B(a)P.

ACKNOWLEDGEMENTS

We thank Pinjie Zhang for assistance with rat breeding. This work was financially supported by the National Natural Science Foundation of China (NSFC21177123;

21407143).

CONFLICT OF INTEREST

The Authors did not report any conflict of interest.

REFERENCE

1 J. Waldman, P. Lioy, A. Greenberg and J. Butler, *J. Expo. Anal. Environ. Epidemiol.*, 1991, **1**, 193-225.

2 H.S. Rosenkranz and R. Mermelstein, *Environ. Carcinog. Rev.*, 1985, **3**, 221-272.

3 H. Jiao, S.L. Allinson, M. J. Walsh, R. Hewitt, K. J. Cole, D. H. Phillips and F. L. Martin, *Mutagenesis*, 2007, **22**, 111-116.

4 C. Fang and Q. Y. Zhang, *J. Pharmacol. Exp. Ther.*, 2010, **334**, 156-163.

5 L. Min, S. He, Q. Chen, F. Peng, H. Peng and M. Xie, *Toxicol. Mech. Methods.*, 2011, **21**, 374-382.

6 D. Kuang, W. Zhang, Q. Deng, X. Zhang, K. Huang, L. Guan, D. Hu, T. Wu and H. Guo, *Environ. Sci. Technol.*, 2013, **47**, 7446-7456.

7 F. Inyang, A. Ramesh, P. Kopsombut, M. S. Niaz, D. B. Hood, A. M. Nyanda and A. E. Archibong, *Reprod. Toxicol.*, 2003, **17**, 527-537.

8 Y. Zhao, X. Chen, X. Liu, Y. Ding, R. Gao, Y. Qiu, Y. Wang and J. He, *Food Chem. Toxicol.*, 2014, **69**, 244-251.

9 C. Casals-Casas and B. Desvergne, *Annu. Rev. Physiol.*, 2011, **73**, 135-162.

10 N. Verma, M. Pink, A.W. Rettenmeier and S. Schmitz-Spanke, *J. Proteomics*, 2013, **85**, 53-64.

11 X. Lu, J. Shao, H. Li and Y. Yu, *Genomics*, 2009, **93**, 332-342.

12 A. I. Malik, A. Williams, C. L. Lemieux, P. A. White and C. L. Yauk, *Environ. Mol. Mutagen.*, 2012, **53**, 10-21.

13 S. I. Jeong, S. E. Lee, H. Yang, C. S. Park, J. J. Cho and Y. S. Park, *Biochip J.*

2012, **6**, 191-196.

14 J. J. Michaelson, S. Trump, S. Rudzok, C. Gräbsch, D. J. Madureira, F. Dautel, J. Mai, S. Attinger, K. Schirmer and M. von Bergen, *BMC genomics*, 2011, **12**, 502.

15 J. L. Griffin, L. A. Walker, J. Troke, D. Osborn, R. F. Shore and J. K. Nicholson, *FEBS LETT.*, 2000, **478**, 147-150.

16 M. R. Viant and U. Sommer, *Metabolomics*, 2013, **9**, 144-158.

17 L. Zhang, X. Liu, L. You, D. Zhou, Q. Wang, F. Li, M. Cong, L. Li, J. Zhao and D. Liu, *Environ. Toxicol. Pharmacol.*, 2011, **32**, 218-225.

18 T. D. Williams, H. Wu, E. M. Santos, J. Ball, I. Katsiadaki, M. M. Brown, P. Baker, F. Ortega, F. Falciani and J. A. Craft, *Environ. Sci. Technol.*, 2009, **43**, 6341-6348.

19 S. A. Brown, A. J. Simpson and M. J. Simpson, *Environ. Chem.*, 2009, **6**, 432-440.

20 O. A. Jones, D. J. Spurgeon, C. Svendsen and J. L. Griffin, *Chemosphere*, 2008, **71**, 601-609.

21 B. P. Lankadurai, D. M. Wolfe, A. J. Simpson and M. J. Simpson, *Environ. Pollut.*, 2011, **159**, 2845-2851.

22 S. Uno, T. P. Dalton, S. Derkenne, C. P. Curran, M. L. Miller, H. G. Shertzer and D. W. Nebert, *Mol. Pharmacol.*, 2004, **65**, 1225-1237.

23 G. Csaba, A. Inczefi-Gonda and S. Szeberenyi, *Gen. Pharmacol.*, 1991, **22**, 815-818.

24 A. M. De Livera, D. A. Dias, D. De Souza, T. Rupasinghe, J. Pyke, D. Tull, U.

Roessner, M. McConville and T. P. Speed, *Anal. Chem.*, 2012, **84**, 10768-10776.

25 S. Bijlsma, I. Bobeldijk, E. R. Verheij, R. Ramaker, S. Kochhar, I. A. Macdonald, B. van Ommen and A. K. Smilde, *Anal. Chem.*, 2006, **78**, 567-574.

26 J. Zhang, L. Yan, W. Chen, L. Lin, X. Song, X. Yan, W. Hang and B. Huang, *Anal. Chim. Acta.*, 2009, **650**, 16-22.

27 J. Zhang, L. Yan, M. Tian, Q. Huang, S. Peng, S. Dong and H. Shen, *J. Pharm. Biomed. Anal.*, 2012, **66**, 287-297.

28 E. C. Chan, K. K. Pasikanti and J. K. Nicholson, *Nat. Protoc.*, 2011, **6**, 1483-1499.

29 C. M. Lee, S. Y. Chen, Y. C. Lee, C. Y. Huang and Y. M. Chen, *Toxicol. Appl. Pharmacol.*, 2006, **214**, 126-135.

30 Y. Qiu, B. Zhou, M. Su, S. Baxter, X. Zheng, X. Zhao, Y. Yen and W. Jia, *Int. J. Mol. Sci.*, 2013, **14**, 8047-8061.

31 L. A. Taylor, J. Arends, A. K. Hodina, C. Unger and U. Massing, *Lipids Health Dis.*, 2007, **6**, 1-8.

32 Y. Su, B. Zhao, F. Guo, Z. Bin, Y. Yang, S. Liu, Y. Han, J. Niu, X. Ke, N. Wang, X. Geng, C. Jin, Y. Dai and Y. Lin, *Ann. Epidemiol.*, 2014, **24**, 98-103.

33 N. V. Reo, M. Adinehzadeh and B. D. Foy, *Biochim. Biophys. Acta.*, 2002, **1580**, 171-188.

34 T. L. Smith, S. T. Merry, D. L. Harris, F. J. Joe, J. Ike, A. E. Archibong and A. Ramesh, *Toxicol. In Vitro.*, 2007, **21**, 753-758.

35 L. N. Vandenberg, T. Colborn, T. B. Hayes, J. J. Heindel, D. R. Jacobs, D. H. Lee,

T. Shioda, A. M. Soto, F. S. vom Saal and W. V. Welshons, *Endocr. Rev.*, 2012, **33**, 378-455.

36 S. Tian, L. Pan and H. Zhang, *Mar. Environ. Res.*, 2014, **94**, 7-15.

37 L. Yuan, J. Zha, Z. Wang, W. Wang, W. Wang, L. Li and L. Zhu, *Chemosphere*, 2013, **93**, 209-216.

38 N. Verma, M. Pink, A. W. Rettenmeier and S. Schmitz‐Spanke, *Proteomics*, 2012, **12**, 1731-1755.

39 B. M. Kim, J. S. Rhee, C. B. Jeong, S. J. Lee, Y. S. Lee, I. Y. Choi and J. S. Lee, *Aquat. Toxicol.*, 2014, **152**, 232-243.

40 A. Kehlen, N. Englert, A. Seifert, T. Klonisch, H. Dralle, J. Langner and C. Hoang-Vu, *Int. J. Cancer.*, 2004, **109**, 833-838.

41 S. Kadekar, I. Silins, A. Korhonen, K. Dreij, L. Al-Anati, J. Högbergand and U. Stenius, PLoS One, 2012, **7**, e43209.

42 E. Tøsti, L. Dahl, M. Endresen and T. Henriksen, *Scand. J. Clin. Lab. Invest.* 1999, **59**, 249-257.

43 P. L. Grover and F. L. Martin, *Carcinogenesis.* 2002, **23**, 1095-1102.

44 X. Tekpli, M. Rissel, L. Huc, D. Catheline, O. Sergent, V. Rioux, P. Legrand, J.A. Holme, M. T. Dimanche-Boitrel and D. Lagadic-Gossmann, *Toxicol. Appl. Pharmacol.*, 2010, **243**, 68-76.

45 M. Gorria, X. Tekpli, O. Sergent, L. Huc, F. Gaboriau, M. Rissel, M. Chevanne, M. T. Dimanche-Boitrel and D. Lagadic-Gossmann, *Ann. N. Y. Acad. Sci.*, 2006, **1090**, 108-112.

46 B. L. Upham, L. Blåha, P. Babica, J. S. Park, I. Sovadinova, C. Pudrith, A. M. Rummel, L. M. Weis, K. Sai, P. K. Tithof, M. Guzvić, J. Vondrácek, M. Machala and J. E. Trosko, *Cancer. Sci.*, 2008, **99**, 696-705.

47 B. Sadikovic and D. I. Rodenhiser, *Toxicol. Appl. Pharmacol.*, 2006, **216**, 458-468.

48 J. Corrales, X. Fang, C. Thornton, W. Mei, W. B. Barbazuk, M. Duke, B. E. Scheffler and K. L. Willett, *Comp. Biochem. Physiol. C. Toxicol. Pharmacol.*, 2014, **163**, 37-46.

49 N. Bhutani, D. M. Burns and H. M. Blau, *Cell.* 2011, **146**, 866-872.

50 A. S. Ptolemy and N. Rifai, *Scand. J. Clin. Lab. Invest. Suppl.*, 2010, **242**, 6-14.

452 **FIGURE LEGENDS:**

453

454 **Figure 1.** Scoring plots of PCA (A) and PLS-DA (B) analysis. ■ control; ● low dose
455 group; ♦ medium dose group.

456

457 **Figure 2.** B(a)P-induced disruption of glycerophospholipid homeostasis in rats. All
458 the data were expressed as mean ± standard deviation (SD). *p< 0.05, **p< 0.01.

459

460 **Figure 3.** B(a)P-induced disruption of sphingolipid homeostasis in rats. All the data
461 were expressed as mean ± standard deviation (SD). *p< 0.05, **p< 0.01.

462

463 **Figure 4.** A schematic representation of the reactions of potential biomarkers involved
464 in glycerophospholipid metabolism and sphingolipid metabolism. PC can be derived
465 from phosphatidylethanolamine catalyzed by phosphatidylethanolamine
466 N-methyltransferase (*pemt*) or the CDP-choline pathway catalyzed by a final-step
467 enzyme choline phosphotransferase (*chpt*). Meanwhile, PC is hydrolyzed by
468 phospholipase A 2 (*pla2*) to generate free fatty acid and LysoPC. The latter can be
469 converted back to PC in the presence of acy-CoA by lysophosphatidylcholine
470 acyltransferase 1/2 (*lpcat1/2*). Besides that, LysoPC is hydrolyzed by *enpp2* to
471 lysophosphatidic acids. Sphingomelin (SM) is mainly regulated by sphingomyelin
472 synathase (*sms*) and sphingomyelin phosphodiesterase (*smpd*, also known as
473 sphingomyelinase). Through the action of either acid or neutral sphingomyelinase,

474 sphingomylein is hydrolyzed to ceramide and phosphocholine. Also, ceramide can be
475 synthesized from sphinganine via *de novo* pathway.
476
477 **Figure 5.** Effects of B(a)P exposure on mRNA expression in rat liver. All the data
478 were expressed as mean ± standard deviation (SD). *p< 0.05, **p< 0.01.

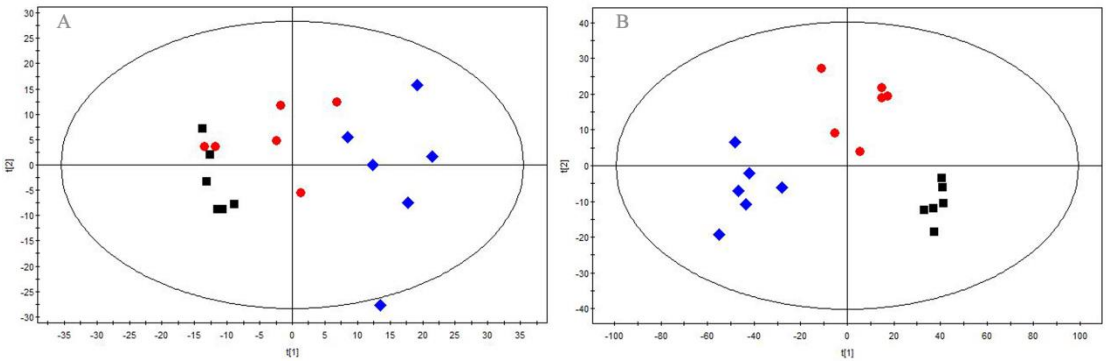

Figure 1. Scoring plots of PCA (A) and PLS-DA (B) analysis. ■ control; ● low dose group; ♦ medium dose group.

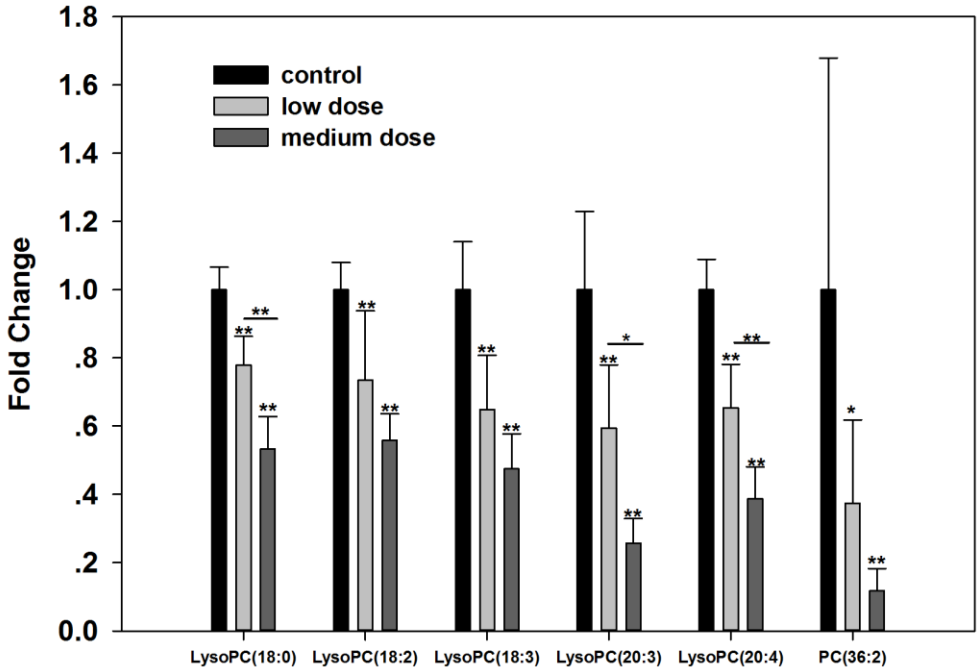

482

483 **Figure 2.** B(a)P-induced disruption of glycerophospholipid homeostasis in rats. All

484 the data were expressed as mean ± standard deviation (SD). *p< 0.05, **p< 0.01.

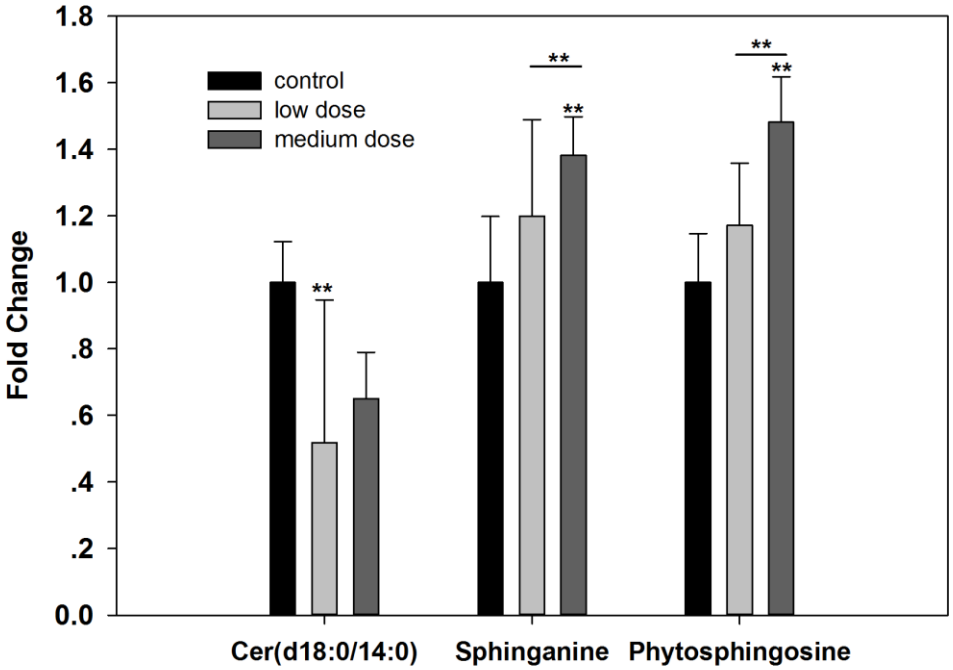

485

486 **Figure 3.** B(a)P-induced disruption of sphingolipid homeostasis in rats. All the data

487 were expressed as mean ± standard deviation (SD). *p< 0.05, **p< 0.01.

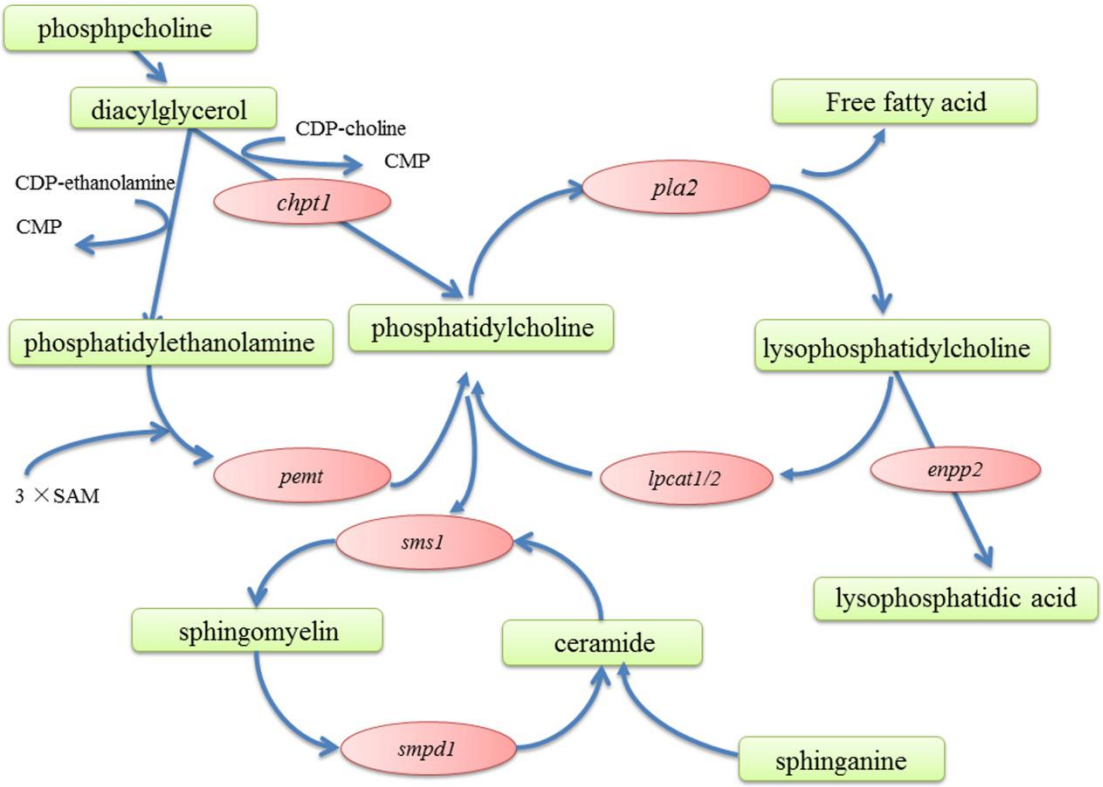

488

489 **Figure 4.** A schematic representation of the reactions of potential biomarkers involved
490 in glycerophospholipid metabolism and sphingolipid metabolism. PC can be derived
491 from phosphatidylethanolamine catalyzed by phosphatidylethanolamine
492 N-methyltransferase (*pemt*) or the CDP-choline pathway catalyzed by a final-step
493 enzyme choline phosphotransferase (*chpt*). Meanwhile, PC is hydrolyzed by
494 phospholipase A 2 (*pla2*) to generate free fatty acid and LysoPC. The latter can be
495 converted back to PC in the presence of acy-CoA by lysophosphatidylcholine
496 acyltransferase 1/2 (*lpcat1/2*). Besides that, LysoPC is hydrolyzed by *enpp2* to
497 lysophosphatidic acids. Sphingomelin (SM) is mainly regulated by sphingomyelin
498 synathase (*sms*) and sphingomyelin phosphodiesterase (s*mpd*, also known as
499 sphingomyelinase). Through the action of either acid or neutral sphingomyelinase,
500 sphingomylein is hydrolyzed to ceramide and phosphocholine. Also, ceramide can be

501 synthesized from sphinganine via *de novo* pathway.

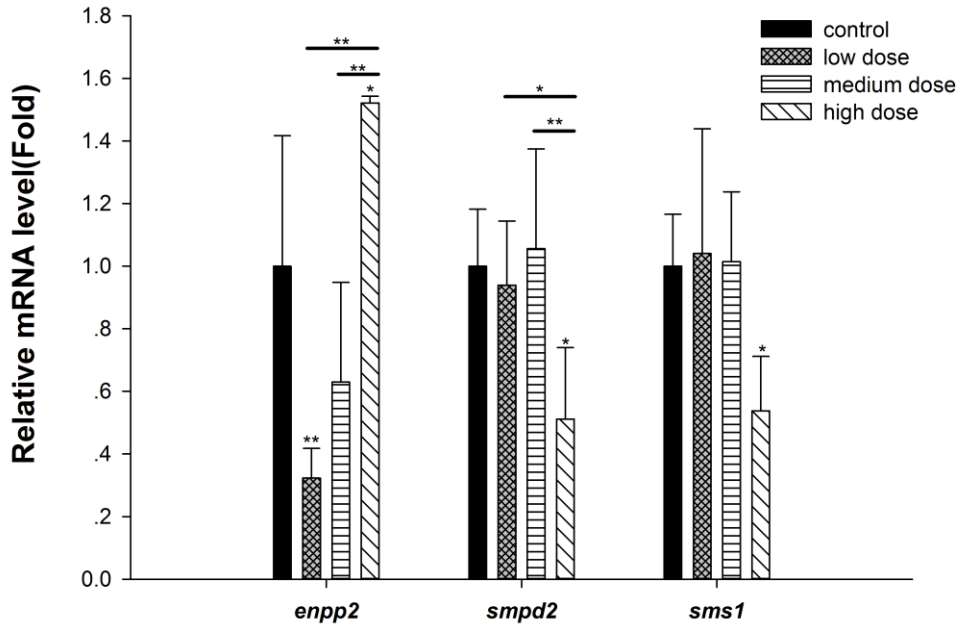

502

503 **Figure 5.** Effects of B(a)P exposure on mRNA expression in rat liver. All the data

504 were expressed as mean ± standard deviation (SD). *p< 0.05, **p< 0.01.

505

506 **Table 1.** Primers sequences used for real-time PCR analysis.

Gene	Full name	Forward primer(5'-3')	Reverse primer(5'-3')
chpt1	choline phosphotransferase	TGGCTATCGGTGCTTCAA	TTCCAAATCGCAACACTCCT
pemt	phosphatidylethanolamine N-methyltransferase	CCATTTCCTTCTGGTTCTGG	CTCTGCTCCCACCTTGCTAC
lpcat1	lysophosphatidylcholine acyltransferase 1	TGGCGGTGAGATAGACCTTC	TCAATAGCCTGGAACAAGTCG
lpcat2	lysophosphatidylcholine acyltransferase 2	GGCCCTTTGCTGTAATCTCA	TAGCCACCTTTCCTTTCACG
enpp2	ectonucleotide pyrophosphatase/phosphodiesterase 2	CCTTCAGTCCGAGTTTGACC	GCCGTCCATACAGGAGATGT
pla2	phospholipase A2	GTCACCAACTTGTTCTCAAACCCAT	CAACTCCACCAGAATCTCACT
sms1	sphingomyelin synathase	CAGGAAGCCAAGATGAGGAG	ACAAGATGGTCAGGGCAGTT
smpd2	sphingomyelin phosphodiesterase	GTTCATCCACCACACATCCA	CCACTCTTTCAGTAGGCAGCA

507 **Table 2. Potential biomarkers of toxicity induced by benzo(a)pyrene.**

No.	HMDB ID	Metabolite	Chemical formula	VIP	Multiple comparisons	*p* value control VS low dose group	*p* value control VS medium dose group	Sub-Pathway	KEGG Pathway
1	HMDB10384	LysoPC(18:0)	C26H54NO7P	7.28	0.001	0.004	0.006	Glycerophospholipid metabolism	Lipid metabolism
2	HMDB10386	LysoPC(18:2)	C26H50NO7P	5.28	0.016	0.055	0.006		
3	HMDB10395	LysoPC(20:4)	C28H50NO7P	4.84	0.001	0.004	0.006		
4	HMDB10393	LysoPC(20:3)	C28H52NO7P	2.04	0.001	0.006	0.006		
5	HMDB10387	LysoPC(18:3)	C26H48NO7P	1.79	0.004	0.006	0.006		
6	HMDB08299	PC(36:2)	C44H84NO8P	3.63	0.004	0.037	0.006		
7	HMDB12273	Palmitic amide	C16H33NO	2.16	0.024	0.262	0.011	Fatty acid metabolism	
8	HMDB00269	Sphinganine	C18H39NO2	3.54	0.01	0.2	0.006	Sphingolipid metabolism	
9	HMDB04610	Phytosphingosine	C18H39NO3	2.98	0.004	0.15	0.006		
10	HMDB11759	Cer(d18:0/14:0)	C32H65NO3	2.58	0.014	0.025	0.006		
11	HMDB00883	Valine	C5H11NO2	3.19	0.002	0.01	0.006	Valine, leucine and isoleucine degradation/ biosynthesis	Amino acid metabolism
12	HMDB00630	Cytosine	C4H5N3O	2.6	0.011	0.423	0.011	Pyrimidine metabolism	Nucleotide metabolism